ACS MEASUREMENT SCIENCE Au
AN OPEN ACCESS JOURNAL OF THE AMERICAN CHEMICAL SOCIETY

pubs.acs.org/measureau

Article

Real-Time Reaction Monitoring of Azide−Alkyne Cycloadditions Using Benchtop NMR-Based Signal Amplification by Reversible Exchange (SABRE)

Hye Jin Jeong, Sein Min, Juhee Baek, Jisu Kim, Jean Chung, and Keunhong Jeong*

Cite This: *ACS Meas. Sci. Au* 2023, 3, 134−142

Read Online

ACCESS | Metrics & More | Article Recommendations | Supporting Information

ABSTRACT: Rufinamide, possessing a triazole ring, is a new antiepileptic drug (AED) relatively well-absorbed in the lower dose range (10 mg/kg per day) and is currently being used in antiepileptic medications. Triazole derivatives can interact with various enzymes and receptors in biological systems via diverse non-covalent interactions, thus inducing versatile biological effects. Strain-promoted azide−alkyne cycloaddition (SPAAC) is a significant method for obtaining triazoles, even under physiological conditions, in the absence of a copper catalyst. To confirm the progress of chemical reactions under biological conditions, research on reaction monitoring at low concentrations is essential. This promising strategy is gaining acceptance for applications in fields such as drug development and nanoscience. We investigated the optimum Ir catalyst and magnetic field for achieving maximum proton hyperpolarization transfer in triazole derivatives. These reactions were analyzed using signal amplification by reversible exchange (SABRE) to overcome the limitations of low sensitivity in nuclear magnetic resonance spectroscopy, when monitoring copper-free click reactions in real time. Finally, a more versatile copper-catalyzed click reaction was monitored in real time, using a 60 MHz benchtop NMR system, in order to analyze the reaction mechanism.

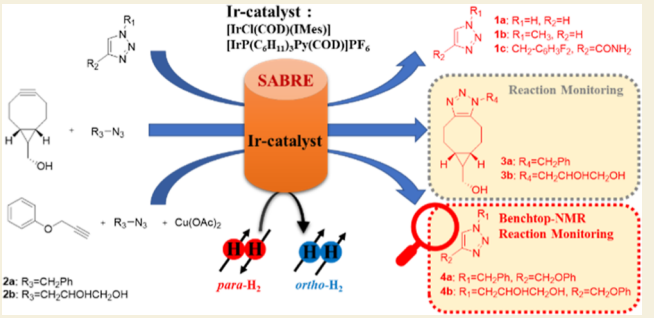

KEYWORDS: *NMR, hyperpolarization, signal amplification by reversible exchange, triazole, reaction monitoring*

INTRODUCTION

Epilepsy is characterized by treatment-resistant seizures and causes a high rate of seizure-related injury. Many patients with epilepsy continue to have seizures despite treatment with currently available antiepileptic drugs (AEDs), which include valproic acid, lamotrigine, topiramate, and felbamate and work by decreasing abnormal excitement in the brain.[1,2] Rufinamide (**1a**) is a new, orally active AED, which is relatively well absorbed in the lower dose range and contains a triazole structure.[3] Triazole derivatives possess a range of pharmacological activities, for example, anti-microbial,[4,5] anti-cancer,[6] analgesic,[7] and antiviral activities.[8]

Classically, the general procedure for producing triazole derivatives involves "click chemistry," that is, the utilization of a copper(I)-catalyzed azide−alkyne cycloaddition (CuAAC) to produce small molecules with heteroatom links (C−N).[9,10] It is generally a high-yielding chemical reaction that produces easily removable side products, under relatively mild conditions. CuAAC is used for bioconjugation to produce fluorophores and reporter molecules.[11−13]

Strain-promoted azide−alkyne cycloaddition (SPAAC) can be carried out using cyclooctyne, which can be effectively converted to a triazole without using a copper catalyst. SPAAC has been recognized for its ability to selectively modify biomolecules and living cells under physiologically plausible conditions.[11−13] Bicyclo[6.1.0]-nonyne (BCN) demonstrated exceptional reactivities in a copper-free click reaction with various azides.[14,15]

Based on the prevalence of triazoles in biologically active molecules, a more fundamental understanding of the chemistry involved in the production process is required in order to aid their utilization in pharmaceuticals. Nuclear magnetic resonance (NMR) spectroscopy has been used extensively to develop a detailed understanding of reaction mechanisms through real-time monitoring.[16,17] The benefit of this strategy is that it allows easy tracking of the species in question, assuming that there are separate signals across a specific region.[18,19] However, classical NMR spectroscopy incurs significant startup, operating, and maintenance costs due to the superconducting magnet technology, thereby limiting its

Received: November 14, 2022
Revised: December 30, 2022
Accepted: January 3, 2023
Published: January 10, 2023

https://doi.org/10.1021/acsmeasuresciau.2c00065
ACS Meas. Sci. Au 2023, 3, 134−142

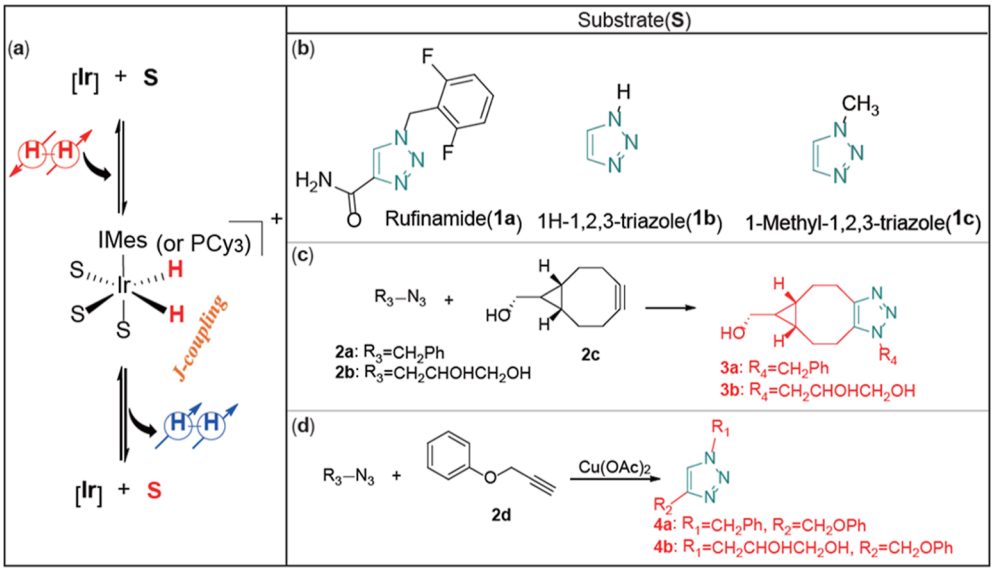

Figure 1. (a) Overall scheme for the SABRE-based hyperpolarization; (b) triazole derivatives as a substrate in SABRE experiments; (c) scheme of SPAAC for real-time monitoring using hyperpolarization in 300 MHz NMR; and (d) scheme of CuAAC for real-time monitoring using hyperpolarization in 60MHz NMR.

application range. Benchtop NMR spectroscopic analysis uses small permanent magnets and is, therefore, less expensive. It is also more useful for studying pharmacokinetics and pharmacodynamics of drug targets, commonly analyzed in the medical and drug discovery sectors.[20−22] However, real-time reaction monitoring using bench-top NMR at low concentrations is difficult to measure without a multi-scan in a short time due to low resolution. Recently, applying hyperpolarization has attracted the attention of chemists for being one of the most promising methods for overcoming this limitation. Hyperpolarization techniques have been developed and applied to many types of chemical compounds, including small molecules and biomedical materials.[23−27] Brute force polarization,[28] dynamic nuclear polarization (DNP),[29−31] spin-exchange optical pumping (SEOP),[32,33] parahydrogen-induced polarization (PHIP),[34−36] and signal amplification by reversible exchange (SABRE)[37−39] are all examples of hyperpolarization techniques. The parahydrogen-based hyperpolarization technique has been widely considered to have the greatest potential as a reaction monitoring tool for real-time reactions.[40,41] Further, SABRE, rather than PHIP using hydrogenation, has been confirmed as a potential mechanism for reaction monitoring and shows promise for future MRI applications.[42,43]

METHODS

Materials and Methods

Sample Preparation. Chemicals (**1a−1c** and **2a−2d**) and deuterated solvents (methanol-d_4, CD_3OD, 99.8 atom %D, Eurisotop, and dimethyl sulfoxide-d_6, CD_3SOCD_3, 99.8 atom %D, Eurisotop) were also used in the form obtained. In the experiment, pre-catalysts {[Ir(IMes) (COD)Cl] and [Ir(COD) (PCy_3) (py)]PF_6)] (2 mg, 3.1 μmol)} and substrates (**1a−1c**, **3a−3b**, and **4a-4b**, 31 μmol) were dissolved in a deuterated solvent (900 μL).

SABRE Catalyst Activation and Calculation of the Hyperpolarized Signal

^{1}H NMR spectra used for the characterization of **1a−1c**, **2a−2d**, and **3a−3b** were acquired on a Bruker Avance III NMR spectrometer operating at ^{1}H resonance frequencies of 300 and 60 MHz. The *para*-hydrogen generator was composed of a home-built instrument, in which hydrogen gas (Hanmi gas, >99.9%, a mixture of the spin isomers ortho-hydrogen and *para*-hydrogen) was allowed to pass through a heat exchanger filled with a FeO(OH) catalyst (Sigma-Aldrich). This instrument was filled with liquid nitrogen in a Dewar flask generating ca. 50% *para*-hydrogen. **1a−1c** (31 μmol) was added to a solution of pre-catalysts (3.1 μmol) in methanol-d_4 or MeOD:DMSO-d_6 = 2:1, individually. A continuous flow of *para*-hydrogen was allowed into the reactants and catalyst mixture at a rate of 6 mL/min at 23 °C and 1 atm. In order to activate a mixture of the substrate and the catalyst, *para*-hydrogen was bubbled through the sample for 20 min in the NMR tube under the earth's magnetic field. Samples were injected rapidly into a 300 MHz NMR and 80 MHz spectrometer, in less than 5 s, to measure the hyperpolarized signals. Measurements were taken in a multitude of magnetic fields (the earth's magnetic field, 30 G, 50 G, 70 G, 90 G, 110 G, and 130 G), and signals of hyperpolarized hydrogen were regularly obtained. All NMR spectra were obtained for each magnetic field by bubbling for another 1 min and taking one scan. Detailed experimental processes were conducted in the same manner as that mentioned in the refs 26 39, and 41.

Click Reaction Monitoring using SABRE Hyperpolarization

For SPAAC reaction monitoring, pre-catalysts (0.07 μmol), reactants (**2a** and **2c**, 0.7 μmol) were dissolved in methanol-d_4 (900 μL). The reaction mixture was transferred to a 5 mm NMR tube and activated by *para*-hydrogen for 20 min in a 90 G magnetic field. The bubbling process by *para*-hydrogen substituted the stirring of the solution. After activation, an individual hyperpolarized spectrum was obtained by using the same hyperpolarized signal measurement procedure as that described above, using 300 MHz NMR, at 10 min intervals over 2 h. In the case of benchtop reaction monitoring via hyperpolarization, pre-catalysts (2 mg, 3.1 μmol) and reactants (**2a**, **2b**, and **2d**, 31 μmol) were dissolved in deuterated solvents (900 μL). The reaction monitoring process was conducted in the same manner as that mentioned above, using 60 MHz NMR, at min intervals over 2 h.

Synthesis of 3a and 3b

((5aR,6aS)-1-Benzyl-1,4,5,5a,6,6a,7,8-octahydrocyclopropa-[5,6]cycloocta[1,2-*d*][1,2,3]triazol-6-yl)methanol (3a). (1*R*,8*S*,9*S*)-Bicyclo[6.1.0]non-4-un-9-ylmethanol (**2c**, 24 mg, 0.16 μmol) was added to the solution of benzyl azide (**2a**, 21 mg, 0.16 μmol) in the acetonitrile/water (3:1) mixture and stirred at room temperature for 2 h. The reaction solution was evaporated under

https://doi.org/10.1021/acsmeasuresciau.2c00065
ACS Meas. Sci. Au 2023, 3, 134−142

reduced pressure, and the resulting mixture was diluted with methylene chloride (5 mL). The crude mixture was washed with water (5 mL), dried over magnesium sulfate, and concentrated under reduced pressure. The resulting mixture was confirmed by column chromatography (ethyl acetate, R_f = 0.4). Yield: 45 mg (100%)

3-((5aR,6aS)-6-(Hydroxymethyl)-5,5a,6,6a,7,8-hexahydrocyclopropa[5,6]cycloocta[1,2-*d*][1,2,3]triazol-1(4*H*)-yl)propane-1,2-diol (3b). (1*R*,8*S*,9*S*)-Bicyclo[6.1.0]non-4-un-9-yl-methanol (**2c**, 20 mg, 0.13 μmol) was added to the solution of 3-azido-1,2-propandiol (**2b**, 16 mg, 0.13 μmol) in methanol (1 mL) and stirred at room temperature for 2 h. The reaction solution was evaporated under reduced pressure, and the resulting mixture was diluted with methylene chloride (5 mL). The crude mixture was washed with water (5 mL), dried over magnesium sulfate, and concentrated under reduced pressure. The resulting mixture was confirmed by column chromatography (ethyl acetate, R_f = 0.1). Yield: 36 mg (99%)

Synthesis of 4a and 4b, General Procedure

1-Phenoxy-2-propyne (**2d**, 200 mg, 1.5 mmol) and copper acetate (27 mg, 0.15 mmol) were added to the solution of azide (**2a** and **2b**, 1.5 mmol) in methanol (2 mL) and stirred at room temperature for 2 h. The reaction solution was evaporated under reduced pressure, and the resulting mixture was diluted with methylene chloride (5 mL). The crude mixture was washed with water (5 mL), dried over magnesium sulfate, and concentrated under reduced pressure. The resulting mixture was confirmed by column chromatography (**4a**: 99% and **4b**: 100%).

RESULTS AND DISCUSSION

Parahydrogen and the targeted substrates reversibly coordinate to the metal center of an Ir catalyst. In SABRE (Figure 1a), the magnetic symmetry of parahydrogen is broken, and the bound hydride ligands are able to transfer their enhanced polarization into the substrate via *J*-coupling of the complex.

A wide range of proton hyperpolarization in targeted structures can be expected. Owing to the associated interest and importance, SABRE-based experiments on SPAAC using ^{15}N-containing synthons were recently performed, focusing on ^{15}N nuclei within the structure.[44] However, hyperpolarization can also be delivered to various structural components combined with ^{1}H,[45−47] ^{13}C,[24,48,49] and ^{15}N[44,50] NMR signals; therefore, there is the possibility of observing a wider range of hyperpolarization by also focusing on other NMR-active nuclei.

Therefore, to expand the study and applicability of SABRE, larger bioactive molecules, with various NMR-active nuclei, must be investigated. This can be explored using benchtop NMR reaction monitoring systems.

Since an integrated enhanced signal from NMR after SABRE is not applicable to the quantitative estimation of the reaction, non-uniform signal amplification may not be a perfect method for the reaction monitoring system. However, identifying hidden NMR signals from reaction monitoring can provide structural information from intermediates and/or products, which can be a useful analytical method both in thermodynamic analysis and in kinetic analysis. Therefore, we demonstrated the hyperpolarization of rufinamide, a triazole-containing drug used for epilepsy and other triazole derivatives.

The triazole derivatives produced by SPAAC and CuAAC for bioconjugation were investigated using real-time reaction monitoring of low-concentration samples, focusing on individual protons in order to understand the click reaction mechanism. These protons cannot be detected without hyperpolarization in a single scan and the same magnetic field. We used both Crabtree's Ir catalyst and the IMes-Ir catalyst (Figure S1) to optimize the hyperpolarization conditions. A benchtop 60 MHz NMR system was used to monitor the CuAAC reaction, which provides more versatile triazole structures.

The triazole derivatives produced by SPAAC and CuAAC for bioconjugation were investigated using real-time reaction monitoring of low-concentration samples, focusing on individual protons in order to understand the click reaction mechanism. These protons cannot be detected without hyperpolarization in a single scan and the same magnetic field. We used both Crabtree's Ir catalyst and the IMes-Ir catalyst (Figure S1) to optimize the hyperpolarization conditions. A benchtop 60 MHz NMR system was used to monitor the CuAAC reaction, which provides more versatile triazole structures.

The overall investigative scope of SABRE-based hyperpolarization and its monitoring using benchtop systems is described in [Figure 1b−d]. Hyperpolarization of triazole derivatives was conducted in various external magnetic fields and optimized in a specific magnetic field for the anticonvulsant drug rufinamide (**1a**), 1*H*-1,2,3-triazole, and 1-methyl-1,2,3-triazole (**1b** and **1c**) (Figure 1b). Formation of hyperpolarized triazole derivatives was monitored in low-concentration click reactions, which used the SPAAC reaction of BCN with an azide, in the absence of a copper catalyst (**3a** and **3b**) (Figure 1c). Additionally, benchtop NMR was used to monitor the CuAAC reaction using SABRE hyperpolarization (**4a** and **4b**) (Figure 1d).

The suspected mechanism of rufinamide(**1a**) is a sodium-dependent action with potential limitation, which is considered to have a membrane-stabilizing effect and is the modulation of sodium channel activity.[51,52] In the case of **1a**, the proton of 1 (σ_H 8.4), which contains the aromatic ring, was not the highest amplified proton, as compared to that of **1b** and **1c** (Figure 2a). We assumed that the proton of 1 was affected by the amide group. The proton of **4** was enhanced approximately 25-fold at a magnetic field of 110 G. The maximum amplification of the proton directly connected to aromatic nitrogen was also observed in different triazole derivatives formed through the click reaction. The remote located protons from coordinated nitrogen exhibited reduced signal amplification values similar to those reported previously as 5-fold to 10-fold.[27]

The hyperpolarization of triazole derivativeshas received little attention as the main substrate, and its polarization efficiency of the proton has been reported to be very low or used to as coligand.[53−55] To study the click reaction monitoring, we conducted a SABRE-based hyperpolarization study on several triazole structures to demonstrate its efficacy in hyperpolarization.

Figure 2b shows the ^{1}H thermal and SABRE spectra for 1*H*-1,2,3-triazole (**1b**) with hyperpolarized signal enhancements using the IMes-Ir catalyst at 90 G. The external magnetic field was modified to optimize hyperpolarization; its polarization is maximized at approximately 90 G (Figure S2). The highest amplified proton signal, proton 1 of **1b**, represents a 63-fold hyperpolarization. 1-Methyl-1,2,3-triazole (**1c**) can be used as a co-substrate for several SABRE-compatible substrates.[45,55,56]

We obtained an unprecedented, hyperpolarized signal from the aromatic proton and methyl group of **1c** with an approximately 200-fold enhanced signal after SABRE (Figure 2c). The polarization trend with the magnetic field was maximized at 130 G Aromatic protons 1 and 2 increased to a larger extent than the *N*-methyl group (Figure S2). The

https://doi.org/10.1021/acsmeasuresciau.2c00065
ACS Meas. Sci. Au 2023, 3, 134−142

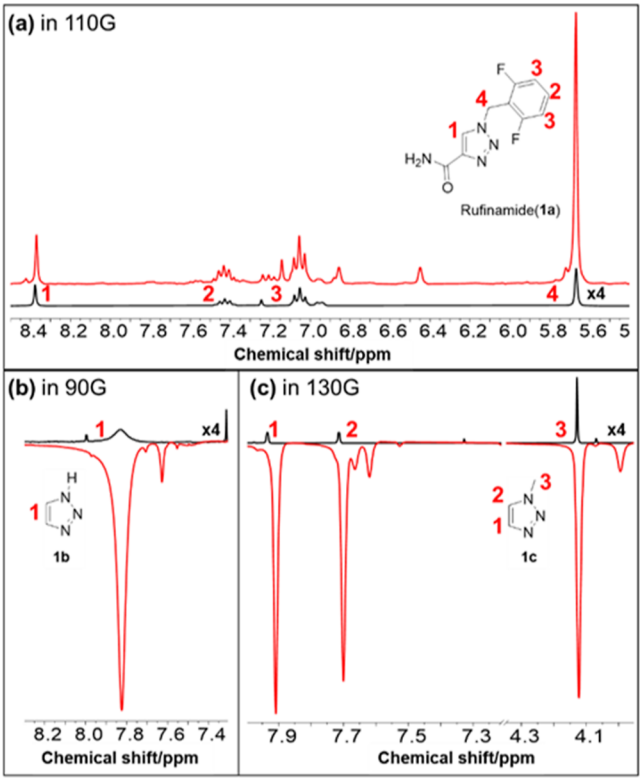

Figure 2. Molecular structures of **1a–c** and the normal ^{1}H NMR (black spectrum) and hyperpolarized signals from **1a–c** (31 μmol) after SABRE in the presence of 110 G, 90 G, and 130 G external magnetic field using the IMes-Ir catalyst (red spectrum).

amplified proton signals were similar across the entire magnetic field. Compared with **1b**, it can be assumed that the electron density of the methyl group aids in stronger binding to the Ir catalyst, resulting in a positive polarization effect.

Unlike **1a**, maximum amplification was observed for the proton directly connected to the aromatic nitrogen, which was also seen in different triazole derivatives formed through the click reaction. After analysis, we concluded that the protons located remotely, that is, away from metal-coordinated nitrogen, exhibited a reduced signal amplification value, which aligns with previously reported data.[27]

After obtaining enough hyperpolarized signals from triazole structures, we proceeded to the next study of click reaction monitoring. The SPACC real-time reaction monitoring system (Figure 3) adopted a low enough concentration of the reactant that fails to identify the whole 3a structure signal from a single scan as an experimental condition. If the number of scans is increased, the 3a structure can be identified even at this low concentration; however, since the signal average with time delay due to the increased number of scans is inevitable, single scan-based real-time reaction monitoring without time delay was carried out after signal amplification through SABRE.

Furthermore, Figures 3 and 4 show plots of different concentrations of 3a, which showed slightly different signal amplification trends in various external magnetic fields (the highest enhancement factor at 90G, 0.7 μmol, Figure S3). The synthesis of triazole derivative **3a** began with azide **2a** (1 eq) and BCN **2c** (1 eq) in the absence of a copper catalyst (Figure 3a). Using the SABRE experiment and **3a** (0.7 μmol), proton (σH 5.5) 1, connected to aromatic nitrogen, exhibited the maximum amplification (approximately 20-fold), and the polarization transfer also proceeded to the neighboring phenyl group, resulting in a 13-fold amplification, as well as an 11-fold amplification of proton 2 at 90 G magnetic field (Figure S3). Notably, regardless of the signal amplification value, the phenyl peaks (σH 7.5) and proton 2 (σH 3.6) were revealed before proton 1 during real-time hyperpolarized monitoring.

Therefore, we can assume that hyperpolarization of the phenyl group is directly caused by parahydrogen in the catalyst, instead of spin diffusion-like polarization transfer from proton 1. Furthermore, based on reaction monitoring, the hyperpolarization effect of proton 1 was assumed to decrease upon nucleophilic attack of a nitrogen anion to the triple bond of BCN because no amplification of reactants was observed at the beginning of the reaction. This perfectly supports the SPAAC mechanism [Figure 3b].

Figure 4 shows the normal signal and its hyperpolarized signal after SABRE with the IMes-Ir catalyst, which demonstrates the extent of hyperpolarization in **3a** from the entire molecular structure. Proton 7, which represents the cyclooctane ring, had the highest amplified signal value in a 110 G magnetic field, among the amplified proton signals. The polarization of the entire structure showed no significant differences, which could be attributed to the fast exchange of the Ir catalyst.

Other than the Zeeman effect and *J*-coupling matching condition, its polarization transfer could be attributed to other factors such as spin diffusion and SPINOE.[57−59] We tested the SABRE method with Crabtree's Ir catalyst, which showed a slightly lower polarization number than the IMes-Ir catalyst. To investigate click reactions in detail, additional reaction monitoring was conducted using SPAAC with 3-azidopropane-1,2-diol to produce **3b**. Similar reaction conditions to the synthesis of **3a** were used, that is, stirring in methanol for 2 h

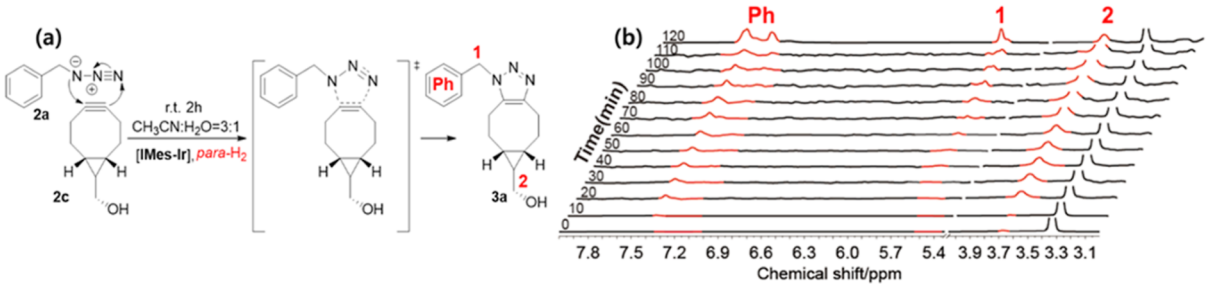

Figure 3. (a) Reaction mechanism for strain-promoted benzyl azide-bicyclo[6.1.0]nonyne (BCN) cycloaddition. (b) ^{1}H spectral reaction monitoring using hyperpolarized SPAAC using benzyl azide (1 eq, 0.7 μmol), BCN (1 eq, 0.7 μmol), and the IMes-Ir catalyst (0.07 μmol) in the presence of a 90 G external magnetic field (300 MHz NMR, 10 min intervals over 2 h).

https://doi.org/10.1021/acsmeasuresciau.2c00065
ACS Meas. Sci. Au 2023, 3, 134−142

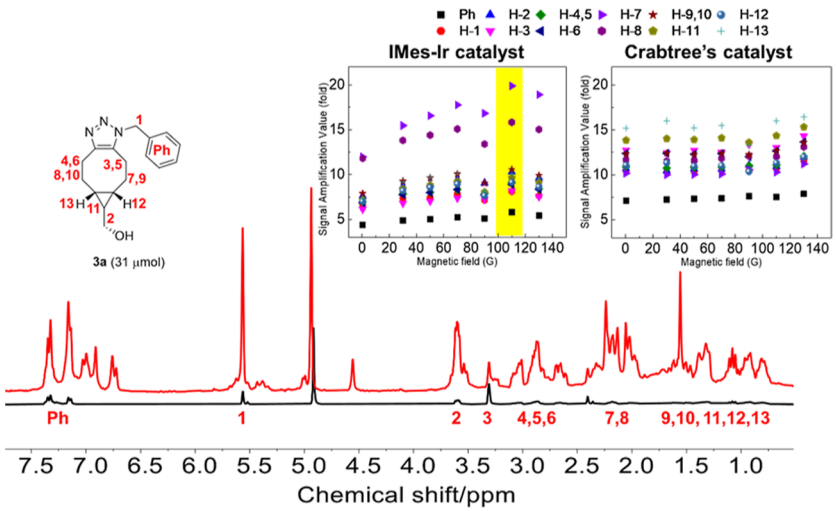

Figure 4. ^{1}H spectrum of **3a** (31 μmol) before (black spectrum) and after SABRE in the presence of 110 G external magnetic field in methanol-d_4 (red spectrum) and signal amplification value of individual protons from hyperpolarized **3a** using the IMes-Ir catalyst and Crabtree's catalyst.

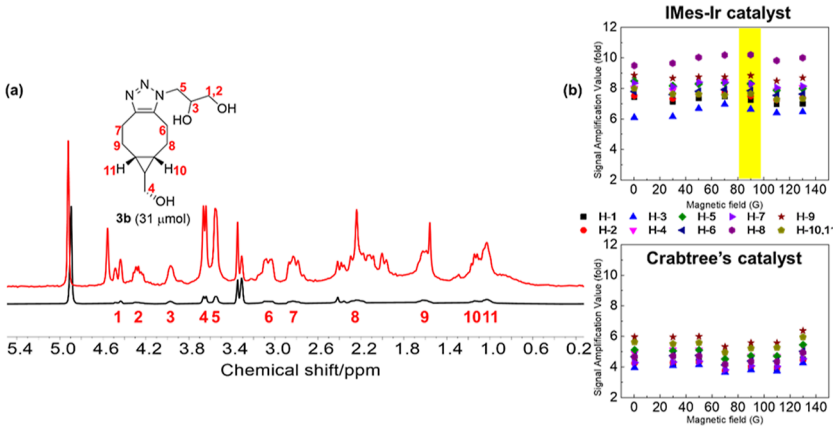

Figure 5. (a) Reaction scheme of strain-promoted 3-azidopropane-1,2-diol-bicyclo[6.1.0]nonyne (BCN) cycloaddition and ^{1}H spectrum of **3b** (31 μmol) before (black spectrum) and after SABRE, in the presence of 90 G external magnetic field, using the IMes-Ir catalyst in methanol-d_4 (red spectrum) and (b) signal amplification value of individual protons from hyperpolarized **3b** using the IMes-Ir catalyst and Crabtree's catalyst.

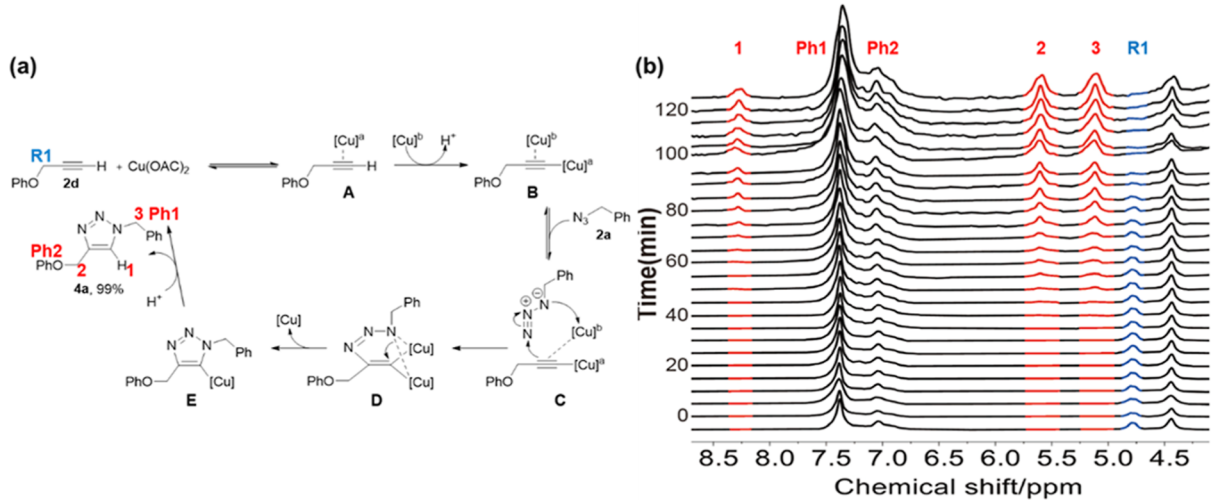

Figure 6. (a) Proposed **2a** and **2d** cycloaddition reaction mechanism, refer to Fokin et. al; (b) ^{1}H spectral reaction monitoring of the hyperpolarized azide−alkyne click reaction in the presence of the earth field using the IMes-Ir catalyst in DMSO-d_6 at 60 MHz NMR.

(Figure 5a). Although **3b** has a lower signal enhancement value than **3a,** it is a triazole structure containing a diol, which can be hyperpolarized using SABRE. Interestingly, the polarization transfer from parahydrogen to **3b** is more efficient than with **3a**

https://doi.org/10.1021/acsmeasuresciau.2c00065
ACS Meas. Sci. Au 2023, 3, 134−142

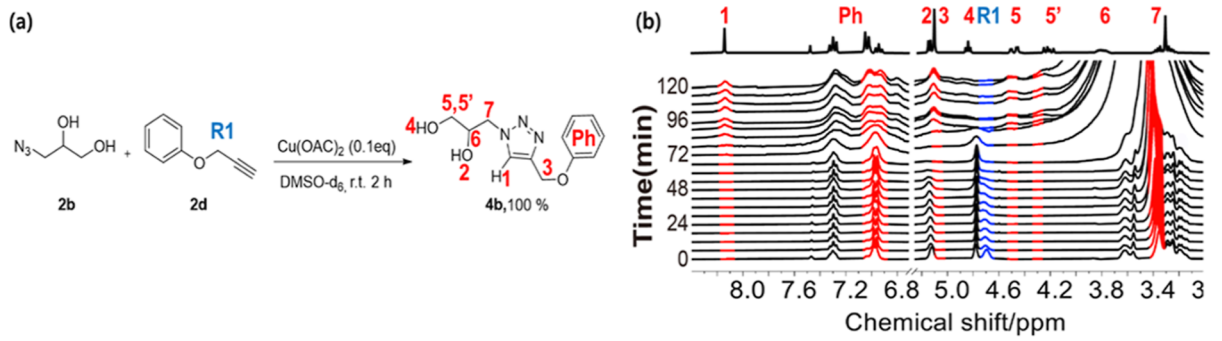

Figure 7. **2b** and **2d** cycloaddition reaction scheme. (b) ^{1}H spectra of the hyperpolarized reaction monitoring azide−alkyne click reaction in the presence of the earth field using the IMes-Ir catalyst in DMSO-d_6 at 60 MHz NMR.

(Figure 5a). The enhancement of **3b** by hyperpolarization was measured while changing the magnetic field during the polarization transfer time (Figure 5b).

However, there was no significant difference in the extent of hyperpolarization across magnetic field strengths. Crabtree's catalyst had lower amplification than the IMes-Ir catalyst, which was similar to **3a**.

A recent study on SPAAC by Ducket's group has revealed that ^{15}N isotope phenyl azide (Ph−$^{15}N_3$) contained long T1 values, enabling strong hyperpolarization when reacting with BCN.[60] It is claimed that these data depict the successful examination of SPAAC reactions as it confirms the possibility of obtaining ^{15}N signals for the phenyl azide and the triazole, simultaneously. Another study presents the hyperpolarization of triazole-containing antifungal drugs and, thus, deducing detailed hyperpolarization mechanisms for both ^{1}H and ^{15}N nuclei.[61] Critically, both signal amplification values in the ^{15}N peaks are increased, but the enhanced ^{1}H signal is similar or lower. The effect is limited to the triazole group, so it was not possible to obtain long-range analysis data.

These SPAAC-based reaction monitoring experiments were performed using a 7 T magnet. Using this setup, we were successful in detecting a hidden structural signal after hyperpolarization.

In contrast, because CuAAC has more potential for producing versatile and simplified triazole structures in reactions, we considered using a portable benchtop NMR as an *in operando* reaction monitoring system. Studying the reaction mechanism of a catalytic reaction is generally more complicated, and it is important to achieve higher reaction efficiency. Real-time CuAAC monitoring was performed using a 60 MHz benchtop NMR and SABRE in DMSO as it is a more bio-friendly solvent, which is less toxic than the methanol solvent and can expect the reaction monitoring in more biological circumstances. Further, its reaction monitoring can expand its possibility to be used in experiments involving many other aprotic solvents. (Figures 6 and 7).

The mechanism showed that the synthesis of **4a** was based on a molecular electron density theory (MEDT) study, using density functional theory (DFT) methods (Figure 6a).[62,63] The formation of intermediate **A** is the first step, whereby 1-phenoxy-2-propyne (**2d**) coordinates to copper acetate. The sigma-bound copper catalyst bearing the pi-bound enriched copper atom **B** reversibly coordinates an organic azide, forming complex **C**. Following this step, a nucleophilic attack at the terminal azido nitrogen by the ß-carbon of the acetylide forms the first covalent C−N bond, producing intermediate **D**. The ligand exchange in this intermediate is faster than the formation of the second covalent C−N bond, which results in ring closure, accounting for the statistical incorporation of Cu into triazolide **E**.

This indicates a thermodynamic preference for the NHC-bound copper triazolide.[62] This reaction can be monitored because of its simple molecular structure through the hydrogen signal amplification of the entire molecule (**4a**) through hyperpolarization. The decreasing number of reactants (R1) and increasing number of products (2 and 3) were clearly observed. Detection of proton 1 was not shown before proton 2 and 3 in SABRE, which supports the theoretical mechanism study that it is formed in the last step of the production of **4a**. Regardless of the progress of the reaction, it is difficult to distinguish the phenyl group, which is present in both the reactant and the product. The amplification of **4a** in methanol is up to 15-fold, and the increase in proton 1 is significant, but monitoring is difficult because deuterium exchange occurs with the deuterated methanol-d_4 solvent during monitoring (Figure S4). Deuterated **4a** was hyperpolarized in methanol-d_4 using 300 MHz NMR. Proton 1 in the triazole ring is deuterated to a significantly lower extent in **4a**. However, it is reported that deuterated substrates have proven beneficial, especially ones able to reduce the number of polarization acceptor spins at the metal center. They also have the additional benefit of attenuating the effect of relaxation.[60]

Signal enhancement is effective for non-deuterated triazole derivatives (Figure S5). Compared with Methanol, DMSO can penetrate biological membranes, such as human skin, affecting the lipid structure and causing bilayer breaks.[64,65] Click reaction monitoring using DMSO and benchtop NMR opens up a new possibility for use in in vitro experiments; it has already been widely used in in vitro drug tests.[66,67]

To track the change of the phenyl group in the click reaction, the synthesis of **4b** was conducted using azido propanediol (Figure 7a). The hyperpolarization of **4b** was inhibited by the diol because the water peak was amplified significantly during the reaction. Figure 7b shows reaction monitoring for the synthesis of **4b**. Noticeably, the change in the phenyl group splitting pattern and the decrease in R1 could also be traced. R1 consumption proceeds faster at 60 min. The slow manifestation of protons 1 and 3 indicates that the reaction rate changes and shows the selectivity of the click reaction. However, it was difficult to observe protons 6 and 7 because of the amplified water peak. Additionally, it is also worth noting that Ir-based SABRE is possible in the copper-containing solvent, allowing for real-time monitoring of the click reaction.

https://doi.org/10.1021/acsmeasuresciau.2c00065
ACS Meas. Sci. Au 2023, 3, 134−142

CONCLUSIONS

Successful real-time click reaction monitoring, which has been widely used in both organic and biological reactions, was performed on a 1.4 T benchtop NMR. SABRE, a real-time hyperpolarization technique, was used to study the reaction mechanism and selectivity and to amplify the hidden proton signals usually undetectable at low concentrations. Furthermore, SABRE studies on several triazole structures, including the drug molecule rufinamide, have revealed much higher hyperpolarization efficiency than previous SABRE studies. These studies provide a wealth of information and potential applications for polarizable biomaterials and also for real-time, SABRE-based benchtop NMR reaction monitoring systems. Eventually, our results may expand the scope of future research to include continuous real-time reaction monitoring and can also be utilized in more biochemical areas, for example, optimizing bio-orthogonal reaction conditions and understanding the reaction mechanisms in confined biological conditions.

ASSOCIATED CONTENT

Supporting Information

The Supporting Information is available free of charge at https://pubs.acs.org/doi/10.1021/acsmeasuresciau.2c00065.

Structures of pre-catalysts, signal amplification value of hyperpolarized **1a**−**1c** at various magnetic fields, signal amplification value of hyperpolarized **3a** at various magnetic fields, reaction scheme of **2a** and **2d** cycloaddition, ^{1}H spectrum of 70% deuterated **4a** before and after SABRE in the presence of earth's field using the IMes-Ir catalyst in methanol and signal amplification value of individual protons from hyperpolarized deuterated **4a** in 300 MHz NMR, and ^{1}H spectrum of **4a** before and after SABRE in the presence of 130 G external magnetic field using the IMes-Ir catalyst in methanol and signal amplification value of individual protons from hyperpolarized **4a** using the IMes-Ir catalyst and Crabtree's catalyst in 300 MHz NMR (PDF)

AUTHOR INFORMATION

Corresponding Author

Keunhong Jeong − *Department of Physics and Chemistry, Korea Military Academy, Seoul 01805, South Korea;* orcid.org/0000-0003-1485-7235; Email: doas1mind@kma.ac.kr

Authors

Hye Jin Jeong − *Department of Chemistry, Colorado State University, Fort Collins, Colorado 80523, United States*

Sein Min − *Department of Chemistry, Seoul Women's University, Seoul 01797, South Korea*

Juhee Baek − *Department of Chemistry, Seoul Women's University, Seoul 01797, South Korea*

Jisu Kim − *Department of Chemistry, Seoul Women's University, Seoul 01797, South Korea*

Jean Chung − *Department of Chemistry, Colorado State University, Fort Collins, Colorado 80523, United States;* orcid.org/0000-0001-8221-0500

Complete contact information is available at: https://pubs.acs.org/10.1021/acsmeasuresciau.2c00065

Author Contributions

H.J.J, S.M, J.B., and J.K. conducted the experiments and analyzed the experimental data. J.C. and K.J. designed the research. H.J.J and K.J. drafted the manuscript.

Funding

This research was supported by the Basic Science Research Program through the National Research Foundation of Korea (NRF) funded by the Ministry of Education (NRF-2021R1A6A3A14046029) and also supported by the National Research Foundation of Korea (NRF) grant funded by the Korean government (MSIT) (No. 2020R1C1C1007888).

Notes

The authors declare no competing financial interest.

REFERENCES

(1) Perucca, E.; Cloyd, J.; Critchley, D.; Fuseau, E. Rufinamide: clinical pharmacokinetics and concentration-response relationships in patients with epilepsy. *Epilepsia* **2008**, *49*, 1123−1141.

(2) Glauser, T.; Kluger, G.; Sachdeo, R.; Krauss, G.; Perdomo, C.; Arroyo, S. Rufinamide for generalized seizures associated with Lennox-Gastaut syndrome. *Neurology* **2008**, *70*, 1950−1958.

(3) Bialer, M.; Johannessen, S. I.; Kupferberg, H. J.; Levy, R. H.; Loiseau, P.; Perucca, E. Progress report on new antiepileptic drugs: a summary of the Fifth Eilat Conference (EILAT V). *Epilepsy Res* **2001**, *43*, 11−58.

(4) Chen, M.; Lu, S.; Yuan, G.; Yang, S.; Du, X. Synthesis and Antibacterial Activity of some Heterocyclic β-Enamino Ester Derivatives with 1,2,3-triazole. *Heterocycl. Commun.* **2000**, *6*, 421−426.

(5) Sheremet, E. A.; Tomanov, R. I.; Trukhin, E. V.; Berestovitskaya, V. M. Synthesis of 4-Aryl-5-nitro-1,2,3-triazoles. *Russ. J. Org. Chem.* **2004**, *40*, 594−595.

(6) Duran, A.; Dogan, H. N.; Rollas, S. Synthesis and preliminary anticancer activity of new dihydro-3-(3-hydroxy-2-naphthyl)-4-substituted-5H-1,2,4-triazoline-5-thiones. *Farmaco* **2002**, *57*, 559−564.

(7) Hafez, H. N.; Abbas, H. A.; El-Gazzar, A. R. Synthesis and evaluation of analgesic, anti-inflammatory and ulcerogenic activities of some triazolo- and 2-pyrazolyl-pyrido[2,3-d]-pyrimidines. *Acta Pharm* **2008**, *58*, 359−378.

(8) Johns, B. A.; Weatherhead, J. G.; Allen, S. H.; Thompson, J. B.; Garvey, E. P.; Foster, S. A.; Jeffrey, J. L.; Miller, W. H. The use of oxadiazole and triazole substituted naphthyridines as HIV-1 integrase inhibitors. Part 1: Estab-lishing the pharmacophore. *Bioorg. Med. Chem. Lett.* **2009**, *19*, 1802−1806.

(9) Kolb, H. C.; Finn, M. G.; Sharpless, K. B. Click Chemistry: Diverse Chemical Function from a Few Good Re-actions. *Angew Chem Int Ed Engl* **2001**, *40*, 2004−2021.

(10) Agard, N. J.; Baskin, J. M.; Prescher, J. A.; Lo, A.; Bertozzi, C. R. A comparative study of bioorthogonal reac-tions with azides. *ACS Chem. Biol.* **2006**, *1*, 644−648.

(11) Codelli, J. A.; Baskin, J. M.; Agard, N. J.; Bertozzi, C. R. Second-generation difluorinated cyclooctynes for copper-free click chemistry. *J. Am. Chem. Soc.* **2008**, *130*, 11486−11493.

(12) Link, A. J.; Vink, M. K. S.; Agard, N. J.; Prescher, J. A.; Bertozzi, C. R.; Tirrell, D. A. Discovery of aminoacyl-tRNA synthetase activity through cell-surface display of noncanonical amino acids. *Proc. Natl. Acad. Sci. U.S.A.* **2006**, *103*, 10180−10185.

(13) Agard, N. J.; Prescher, J. A.; Bertozzi, C. R. A strain-promoted [3 + 2] azide-alkyne cycloaddition for cova-lent modification of biomolecules in living systems. *J. Am. Chem. Soc.* **2004**, *126*, 15046−15047.

(14) Adachi, K.; Meguro, T.; Sakata, Y.; Igawa, K.; Tomooka, K.; Hosoya, T.; Yoshida, S. Selective strain-promoted azide-alkyne cycloadditions through transient protection of bicyclo[6.1.0]nonynes with silver or gold. *Chem Commun (Camb)* **2020**, *56*, 9823−9826.

(15) Dommerholt, J.; Schmidt, S.; Temming, R.; Hendriks, L. J.; Rutjes, F. P.; van Hst, J. C.; Lefeber, D. J.; Friedl, P.; van Delft, F. L. Readily accessible bicyclononynes for bioorthogonal labeling and three-dimensional imaging of living cells. *Angew Chem Int Ed Engl* **2010**, *49*, 9422−9425.
(16) Metz, H.; Mäder, K. Benchtop-NMR and MRI−a new analytical tool in drug delivery research. *Int. J. Pharm.* **2008**, *364*, 170−175.
(17) Kuentz, M.; Rothenhäusler, B.; Röthlisberger, D. Time domain 1H NMR as a new method to monitor soften-ing of gelatin and HPMC capsule shells. *Drug Dev. Ind. Pharm.* **2006**, *32*, 1165−1173.
(18) Burueva, D. B.; Eills, J.; Blanchard, J. W.; Garcon, A.; Picazo-Frutos, R.; Kovtunov, K. V.; Koptyug, I. V.; Budker, D. Chemical Reaction Monitoring using Zero-Field Nuclear Magnetic Resonance Enables Study of Heteroge-neous Samples in Metal Containers. *Angew Chem Int Ed Engl* **2020**, *59*, 17026−17032.
(19) Wu, B.; Ecken, S.; Swyer, I.; Li, C.; Jenne, A.; Vincent, F.; Schmidig, D.; Kuehn, T.; Beck, A.; Busse, F.; Stronks, H.; Soong, R.; Wheeler, A. R.; Simpson, A. Rapid Chemical Reaction Monitoring by Digital Microfluidics-NMR: Proof of Principle Towards an Automated Synthetic Discovery Platform. *Angew Chem Int Ed Engl* **2019**, *58*, 15372−15376.
(20) Zhao, J.; Wang, M.; Avula, B.; Khan, I. A. Detection and quantification of phenethylamines in sports dietary supplements by NMR approach. *J. Pharm. Biomed. Anal.* **2018**, *151*, 347−355.
(21) Gallo, M.; Matteucci, S.; Alaimo, N.; Pitti, E.; Orsale, M. V.; Summa, V.; Cicero, D. O.; Monteagudo, E. A novel method using nuclear magnetic resonance for plasma protein binding assessment in drug discovery programs. *J. Pharm. Biomed. Anal.* **2019**, *167*, 21−29.
(22) Nasr, J. J.; Shalan, S. Validated 1H and 19F nuclear magnetic resonance for the quantitative determination of the hepatitis C antiviral drugs sofosbuvir, ledipasvir, and daclatasvir in tablet dosage forms. *Microchem. J.* **2020**, *152*, 104437.
(23) Hövener, J. B.; Pravdivtsev, A. N.; Kidd, B.; Bowers, C. R.; Glöggler, S.; Kovtunov, K. V.; Plaumann, M.; Katz-Brull, R.; Buckenmaier, K.; Jerschow, A.; Reineri, F.; Theis, T.; Shchepin, R. V.; Wagner, S.; Bhattacharya, P.; Zacharias, N. M.; Chekmenev, E. Y. Parahydrogen-Based Hyperpolarization for Biomedicine. *Angew Chem Int Ed Engl* **2018**, *57*, 11140−11162.
(24) Reineri, F.; Boi, T.; Aime, S. ParaHydrogen Induced Polarization of 13C carboxylate resonance in acetate and pyruvate. *Nat. Commun.* **2015**, *6*, 5858.
(25) Pokochueva, E. V.; Kovtunov, K. V.; Salnikov, O. G.; Gemeinhardt, M. E.; Kovtunova, L. M.; Bukhtiyarov, V. I.; Chekmenev, E. Y.; Goodson, B. M.; Koptyug, I. V. Heterogeneous hydrogenation of phenylalkynes with parahy-drogen: hyperpolarization, reaction selectivity, and kinetics. *Phys. Chem. Chem. Phys.* **2019**, *21*, 26477−26482.
(26) Jeong, H. J.; Min, S.; Jeong, K. Analysis of 1-aminoisoquinoline using the signal amplification by reversible exchange hyperpolarization technique. *Analyst* **2020**, *145*, 6478−6484.
(27) Rakita, A.; Nikolić, N.; Mildner, M.; Matiasek, J.; Elbe-Bürger, A. Re-epithelialization and immune cell be-haviour in an ex vivo human skin model. *Sci. Rep.* **2020**, *10*, 1.
(28) Hirsch, M. L.; Kalechofsky, N.; Belzer, A.; Rosay, M.; Kempf, J. G. Brute-Force Hyperpolarization for NMR and MRI. *J. Am. Chem. Soc.* **2015**, *137*, 8428−8434.
(29) Lawler, R. G. Chemically induced dynamic nuclear polarization. *J. Am. Chem. Soc.* **1967**, *89*, 5519−5521.
(30) Rossini, A. J.; Zagdoun, A.; Lelli, M.; Lesage, A.; Copéret, C.; Emsley, L. Dynamic nuclear polarization sur-face enhanced NMR spectroscopy. *Acc. Chem. Res.* **2013**, *46*, 1942−1951.
(31) Maly, T.; Debelouchina, G. T.; Bajaj, V. S.; Hu, K.-N.; Joo, C.-G.; Mak−Jurkauskas, M. L.; Sirigiri, J. R.; van der Wel, P. C. A.; Herzfeld, J.; Temkin, R. J.; Griffin, R. G. Dynamic nuclear polarization at high magnetic fields. *The journal of chemical physics* **2008**, *128*, 052211−052231.
(32) Walker, T. G.; Happer, W. Spin-exchange optical pumping of noble-gas nuclei. *Rev. Mod. Phys.* **1997**, *69*, 629−642.
(33) Chen, W. C.; Gentile, T. R.; Ye, Q.; Walker, T. G.; Babcock, E. On the limits of spin-exchange optical pump-ing of 3 He. *J. Appl. Phys.* **2014**, *116*, 014903.
(34) Natterer, J.; Bargon, J. Parahydrogen induced polarization. *Prog. Nucl. Magn. Reson. Spectrosc.* **1997**, *31*, 293−315.
(35) Kovtunov, K. V.; Koptyug, I. V.; Fekete, M.; Duckett, S. B.; Theis, T.; Joalland, B.; Chekmenev, E. Y. Parahy-drogen-Induced Hyperpolarization of Gases. *Angew Chem Int Ed Engl* **2020**, *59*, 17788−17797.
(36) Golman, K.; Axelsson, O.; Jóhannesson, H.; Månsson, S.; Olofsson, C.; Petersson, J. S. Parahydrogen-induced polarization in imaging: Subsecond13C angiography. *Magn Reson Med* **2001**, *46*, 1−5.
(37) Rayner, P. J.; Duckett, S. B. Signal Amplification by Reversible Exchange (SABRE): From Discovery to Di-agnosis. *Angew Chem Int Ed Engl* **2018**, *57*, 6742−6753.
(38) Robertson, T. B. R.; Antonides, L. H.; Gilbert, N.; Benjamin, S. L.; Langley, S. K.; Munro, L. J.; Sutcliffe, O. B.; Mewis, R. E. Hyperpolarization of Pyridyl Fentalogues by Signal Amplification By Reversible Exchange (SABRE). *ChemistryOpen* **2019**, *8*, 1375−1382.
(39) Lee, S. J.; Jeong, K.; Shim, J. H.; Lee, H. J.; Min, S.; Chae, H.; Namgoong, S. K.; Kim, K. SQUID-based ul-tralow-field MRI of a hyperpolarized material using signal amplification by reversible exchange. *Sci. Rep.* **2019**, *9*, 12422.
(40) Jeong, K.; Min, S.; Chae, H.; Namgoong, S. K. Monitoring of hydrogenation by benchtop NMR with parahy-drogen-induced polarization. *Magn. Reson. Chem.* **2019**, *57*, 44−48.
(41) Chae, H.; Min, S.; Jeong, H. J.; Namgoong, S. K.; Oh, S.; Kim, K.; Jeong, K. Organic Reaction Monitoring of a Glycine Derivative Using Signal Amplification by Reversible Exchange-Hyperpolarized Benchtop Nuclear Magnetic Resonance Spectroscopy. *Anal. Chem.* **2020**, *92*, 1090210907.
(42) Dücker, E. B.; Kuhn, L. T.; Münnemann, K.; Griesinger, C. Similarity of SABRE field dependence in chemi-cally different substrates. *J. Magn. Reson.* **2012**, *214*, 159−165.
(43) Rayner, P. J.; Burns, M. J.; Olaru, A. M.; Norcott, P.; Fekete, M.; Green, G. G. R.; Highton, L. A. R.; Mewis, R. E.; Duckett, S. B. Delivering strong 1 H nuclear hyperpolarization levels and long magnetic lifetimes through signal amplification by reversible exchange. *Proc. Natl. Acad. Sci. U.S.A.* **2017**, *114*, E3188−E3194.
(44) Rayner, P. J.; Fekete, M.; Gater, C. A.; Ahwal, F.; Turner, N.; Kennerley, A. J.; Duckett, S. B. Real-Time High-Sensitivity Reaction Monitoring of Important Nitrogen-Cycle Synthons by 15N Hyperpolarized Nuclear Magnetic Resonance. *J. Am. Chem. Soc.* **2022**, *144*, 8756−8769.
(45) McCoy, D. E.; Feo, T.; Harvey, T. A.; Prum, R. O. Structural absorption by barbule microstructures of super black bird of paradise feathers. *Nat. Commun.* **2018**, *9*, 1.
(46) Iali, W.; Roy, S. S.; Tickner, B. J.; Ahwal, F.; Kennerley, A. J.; Duckett, S. B. Hyperpolarising Pyruvate through Signal Amplification by Reversible Exchange (SABRE). *Angew. Chem.* **2019**, *131*, 10377−10381.
(47) Zhou, Z.; Yu, J.; Colell, J. F. P.; Laasner, R.; Logan, A.; Barskiy, D. A.; Shchepin, R. V.; Chekmenev, E. Y.; Blum, V.; Warren, W. S.; Theis, T. Long-Lived 13C2 Nuclear Spin States Hyperpolarized by Parahydrogen in Reversi-ble Exchange at Microtesla Fields. *J. Phys. Chem. Lett.* **2017**, *8*, 3008−3014.
(48) Kovtunov, K. V.; Kovtunova, L. M.; Gemeinhardt, M. E.; Bukhtiyarov, A. V.; Gesiorski, J.; Bukhtiyarov, V. I.; Chekmenev, E. Y.; Koptyug, I. V.; Goodson, B. M. Heterogeneous Microtesla SABRE Enhancement of 15 N NMR Signals. *Angew Chem Int Ed* **2017**, *56*, 10433−10437.
(49) Iali, G. A. I. M.; Moustafa, L.; Dagys, S. S.; Roy, S. S. 15 N hyperpolarisation of the antiprotozoal drug ornidazole by Signal Amplification By Reversible Exchange in aqueous medium. *Magn. Reson. Chem.* **2021**, *59*, 1199−1207.
(50) Salnikov, O. G.; Chukanov, N. V.; Svyatova, A.; Trofimov, I. A.; Kabir, M. S. H.; Gelovani, J. G.; Kovtunov, K. V.; Koptyug, I. V.; Chekmenev, E. Y. 15N NMR Hyperpolarization of Radiosensitizing

Antibiotic Nimorazole by Re-versible Parahydrogen Exchange in Microtesla Magnetic Fields. *Angew Chem Int Ed* **2021**, *60*, 2406−2413.
(51) Barskiy, D. A.; Kovtunov, K. V.; Koptyug, I. V.; He, P.; Groome, K. A.; Best, Q. A.; Shi, F.; Goodson, B. M.; Shchepin, R. V.; Truong, M. L.; Coffey, A. M.; Waddell, K. W.; Chekmenev, E. Y. In situ and ex situ low-field NMR spectroscopy and MRI endowed by SABRE hyperpolarization. *ChemPhysChem* **2014**, *15*, 4100−4107.
(52) MacCulloch, K.; Tomhon, P.; Browning, A.; Akeroyd, E.; Lehmkuhl, S.; Chekmenev, E. Y.; Theis, T. Hyperpolarization of common antifungal agents with SABRE. *Magn. Reson. Chem.* **2021**, *59*, 1225−1235.
(53) Arroyo, S. Rufinamide. *Rufinamide. Neurotherapeutics* **2007**, *4*, 155−162.
(54) Wheless, J. W.; Vazquez, B. Rufinamide: a novel broad-spectrum antiepileptic drug. *Epilepsy Curr* **2010**, *10*, 1−6.
(55) Eshuis, N.; Hermkens, N.; van Weerdenburg, B. J. A.; Feiters, M. C.; Rutjes, F. P. J. T.; Wijmenga, S. S.; Tessari, M. Toward nanomolar detection by NMR through SABRE hyperpolarization. *J. Am. Chem. Soc.* **2014**, *136*, 2695−2698.
(56) Adams, R. W.; Aguilar, J. A.; Atkinson, K. D.; Cowley, M. J.; Elliott, P. I. P.; Duckett, S. B.; Green, G. G. R.; Khazal, I. G.; López-Serrano, J.; Williamson, D. C. Reversible interactions with para-hydrogen enhance NMR sensi-tivity by polarization transfer. *Science* **2009**, *323*, 1708−1711.
(57) Glöggler, S.; Emondts, M.; Colell, J.; Müller, R.; Blümich, B.; Appelt, S. Selective drug trace detection with low-field NMR. *Analyst* **2011**, *136*, 1566−1568.
(58) Juriew, J.; Skorochodowa, T.; Merkuschew, J.; Winter, W.; Meier, H. A Simple Route to a New Type of Cy-clophane. *Angew Chem Int Ed Engl* **1981**, *20*, 269−270.
(59) Song, Y. Q. Spin polarization−induced nuclear Overhauser effect: An application of spin-polarized xenon and helium. *Concepts Magn Reson* **2021**, *12*, 6−20.
(60) Marco-Rius, I.; Bohndiek, S. E.; Kettunen, M. I.; Larkin, T. J.; Basharat, M.; Seeley, C.; Brindle, K. M. Quanti-tation of a spin polarization-induced nuclear Overhauser effect (SPINOE) between a hyperpolarized 13C-labeled cell metabolite and water protons. *Contrast Media Mol. Imaging* **2014**, *9*, 182−6.
(61) Navon, G.; Song, Y.-Q.; Rõõm, T.; Appelt, S.; Taylor, R. E.; Pines, A. Enhancement of Solution NMR and MRI with Laser-Polarized Xenon. *Science* **1996**, *271*, 1848−1851.
(62) Ben El Ayouchia, H.; Bahsis, L.; Anane, H.; Domingo, L. R.; Stiriba, S. E. Understanding the mechanism and regioselectivity of the copper(i) catalyzed [3 + 2] cycloaddition reaction between azide and alkyne: a systematic DFT study. *RSC Adv.* **2018**, *8*, 7670−7678.
(63) Worrell, B. T.; Malik, J. A.; Fokin, V. V. Direct evidence of a dinuclear copper intermediate in Cu(I)-catalyzed azide-alkyne cycloadditions. *Science* **2013**, *340*, 457−460.
(64) Anchordoguy, T. J.; Carpenter, J. F.; Crowe, J. H.; Crowe, L. M. Temperature-dependent perturbation of phospholipid bilayers by dimethylsulfoxide. *Biochim. Biophys. Acta* **1992**, *1104*, 117−122.
(65) Barry, B. W. Mode of action of penetration enhancers in human skin. *J Control Release* **1987**, *6*, 85−97.
(66) Santos, N. C.; Figueira-Coelho, J.; Martins-Silva, J.; Saldanha, C. Multidisciplinary utilization of dimethyl sulfoxide: pharmacological, cellular, and molecular aspects. *Biochem. Pharmacol.* **2003**, *65*, 1035−1041.
(67) Colucci, M.; Maione, F.; Bonito, M. C.; Piscopo, A.; Digiannuario, A.; Pieretti, S. New insights of dimethyl sulphoxide effects (DMSO) on experimental in vivo models of nociception and inflammation. *Pharmacol. Res.* **2008**, *57*, 419−425.

https://doi.org/10.1021/acsmeasuresciau.2c00065
ACS Meas. Sci. Au 2023, 3, 134−142